2005

Microdosimetry simulations of solar protons within a spacecraft

A. J. Wroe
University of Wollongong

I. Cornelius
University of Wollongong, iwan@uow.edu.au

Anatoly B. Rosenfeld
University of Wollongong, anatoly@uow.edu.au

V. L. Pisacane
United States Naval Academy, Annapolis, USA

J. F. Zeigler
United States Naval Academy, Annapolis, USA

See next page for additional authors

Authors

A. J. Wroe, I. Cornelius, Anatoly B. Rosenfeld, V. L. Pisacane, J. F. Zeigler, M. E. Nelson, F. Cucinotta, M. Zaider, and J. F. Dicello

Microdosimetry Simulations of Solar Protons Within a Spacecraft

A. J. Wroe, *Student Member, IEEE*, I. M. Cornelius, *Member, IEEE*, A. B. Rosenfeld, *Senior Member, IEEE*,
V. L. Pisacane, J. F. Ziegler, M. E. Nelson, F. Cucinotta, M. Zaider, and J. F. Dicello

Abstract—The microdosimetric spectra derived by silicon microdosimeter in a proton radiation field traversing heterogeneous structures were simulated using the GEANT4 toolkit.

Index Terms—GEANT4, microdosimetry, protons.

I. INTRODUCTION

HUMANS exploring outer space are exposed to space radiation composed of high-energy protons and heavy ions. In deep space, the radiation environment consists mainly of galactic cosmic radiation (GCR). In the energy range from 100 MeV per nucleon to 10 GeV per nucleon, the GCR consists of 87% protons, 12% helium ions, and 1% heavier ions [14]. Protons are also the major component of solar particle events (SPEs), with a smaller contribution from helium and heavier ions emitted from the Sun.

Organizations planning and conducting space travel such as NASA and ESA have a fundamental interest in evaluating adverse health effects induced by GCR and SPEs in human space explorers and their offspring. It is well known that ionizing radiation causes permanent damage to the DNA, which is associated with cancer development and fetal deaths or birth defects. In future space missions both personnel and electronic devices will be required to perform for longer periods within a radiation environment. For these applications it is imperative that heterogeneous shielding structures, biological structures and the secondaries produced by such structures be investigated thoroughly.

The microdosimetric spectra of secondaries can be investigated and monitored utilizing solid-state microdosimeters as have been developed at the CMRP. Currently MIcroDosimetry iNstruments (MIDNs) are employing these silicon microdosimetric sensors as payload on the Midshipman Space

A. J. Wroe, I. M. Cornelius, and A. B. Rosenfeld are with the Centre for Medical Radiation Physics, University of Wollongong, Wollongong, NSW 2087, Australia (e-mail: ajw16@uow.edu.au; iwan@uow.edu.au; anatoly@uow.edu.au).

V. L. Pisacane, J. F. Ziegler, and M. E. Nelson are with the United States Naval Academy, Annapolis, MD 21402 USA (e-mail: pisacane@usna.edu; ziegler@aya.yale.edu; nelson@usna.edu).

F. Cucinotta is with the Radiation Research Department, NASA, Houston, TX USA (e-mail: francis.a.cucinotta@nasa.gov).

M. Zaider is with the Medical Physics Department, Memorial Sloan Kettering Cancer Care Center, New York, NY USA (e-mail: zaiderm@mskcc.org).

J. F. Dicello is with the School of Medicine, Johns Hopkins University, Baltimore, MD USA (e-mail: diceljo@jhmi.edu).

Technology Applications Research (MidSTAR-I) spacecraft under development at the United States Naval Academy [9]. The effectiveness of spacecraft shielding in inhibiting the production of harmful secondaries can also be investigated and in turn optimized utilizing Monte Carlo radiation transport simulation studies. Such programs are already in place, the most notable being the MULASSIS [6] and DESIRE [3] projects. However additional information may be obtained by utilizing dose weighted lineal energy as the measurement parameter.

In this simulation study the GEANT4 Monte Carlo Simulation Toolkit [4] will be used to simulate various layered heterogeneous structures imbedded with the SOI microdosimeter that are irradiated with solar protons. These phantoms will be constructed to reflect a situation present within a space capsule and will simulate the microdosimetric spectra of different phantom configurations. The microdosimetric spectra obtained from these studies will give an indication of the effectiveness of the shielding structures and the microdosimetric spectra at tissue boundaries within the spacecraft capsule. It will also allow for an analysis of the SOI microdosimeter in providing information in real time for spacecraft monitoring.

II. SOLID STATE MICRODOSIMETRY

Solid-state devices providing a true microscopically small sensitive volume (SV) are one option for microdosimetry. The first comparison of microdosimetric measurements between a spherical proportional counter and a single junction solid-state detector were made by Dicello [2]. In this case, a silicon detector of a large area with 7 microns thickness was used. A new approach for silicon microdosimetry based on arrays of silicon SVs (pn-junctions) was proposed by McNulty and Roth [7] for separation of gamma and neutron fields (no microdosimetric spectras was produced) and later SOI microdosimeter was developed and applied to hadron therapy by Rosenfeld [11].

The main advantage of silicon microdosimeters is their compact size and low voltage for operation. However, previously they have suffered the drawback of the lack of a well-defined SV. A new approach to microdosimetry using the silicon on insulator (SOI) technology has been developed at the Centre for Medical Radiation Physics (CMRP) at the University of Wollongong (Fig. 1) and produced by Fujitsu. It comprises a 2D-diode array providing well-defined SVs. This microdosimeter has a significantly improved performance [1]. A SOI microdosimeter, comprising an array of 10^4 silicon cells with a size of 10×10 microns on a single chip with a SV thickness of 2, 5, and 10 microns has been built and was tested at several hadron therapy facilities [12]. Simple scaling of the mean chord length allows
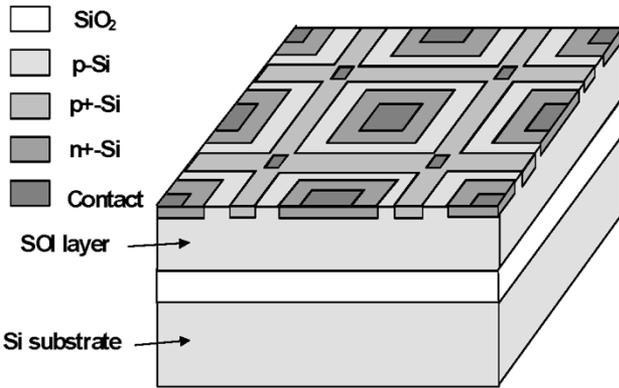
Fig. 1. Basic SOI diode array structure of the microdosimeter used at the CMRP, University of Wollongong.

derivation of tissue-equivalent microdosimetric spectra. The biological dose or RBE of a radiation field can then be determined by convolution of microdosimetric spectra with quality coefficients within the range of lineal energies in a particular radiation field [5].

Preliminary simulations of the energy deposition spectra in a micron-size silicon SV and their comparison with experimental data obtained in neutron and proton fields have shown that such simulations yield useful and accurate information [12]. Simulations can therefore provide an important tool when determining microdosimetric spectra within heterogeneous structures as will be demonstrated in this research.

III. INCIDENT RADIATION SPECTRA

As the goal of this research was to accurately simulate the microdosimetry spectra present in an orbiting satellite it was important to ascertain an accurate incident solar proton radiation spectra. The SPENVIS website [15] would be utilized to generate a solar proton fluence spectra for the international space station. In this case results were obtained for a primarily circular orbit of altitude 360 km and an inclination of $51.6°$ and 12 month mission duration utilizing the JPL model to 95% (Fig. 2).

This model was employed for three conditions; without geomagnetic shielding, accounting for geomagnetic shielding within a stormy magnetosphere, and finally accounting for geomagnetic shielding within a quiet magnetosphere (Fig. 3). In each case a 95% confidence level was maintained.

From these results it was clear that the solar protons were predominantly below 10 MeV in energy, with the maximum energy supplied by the JPL model being 200 MeV. It is well established [13] that solar protons can penetrate much deeper into the magnetosphere than predicted by the simple attenuation model. As the case ignoring geomagnetic shielding was considered a worse-case scenario it would be utilized as the incident proton radiation spectra for our GEANT4 simulations.

IV. MONTE CARLO SIMULATIONS

The GEANT4 Monte Carlo Toolkit was used to simulate the microdosimeric spectra obtained when irradiated with the spectra of solar protons. There were three important components of this program:
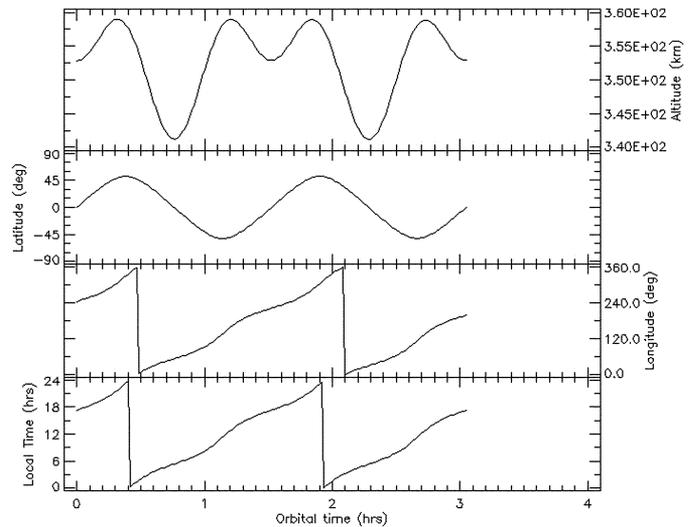

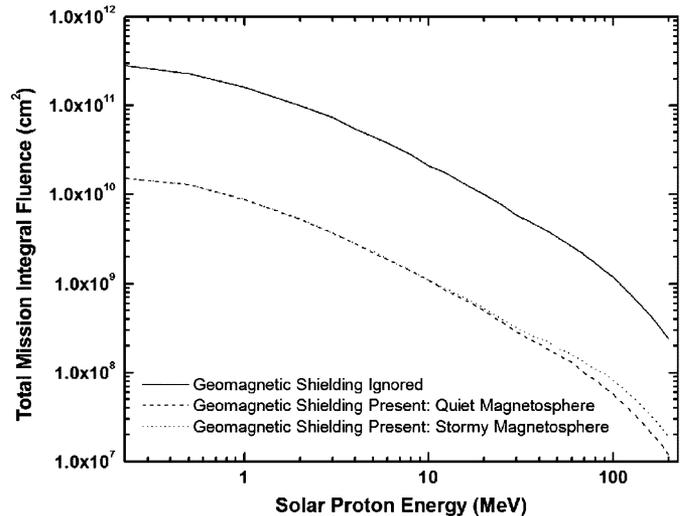Fig. 2. Orbit parameters for two complete orbits of Earth totaling 3 hours 16 minutes.

Fig. 3. Solar proton fluence distributions generated using the JPL model to 95% confidence levels within SPENVIS [15].

- phantom construction and definition;
- physics process and incident particles;
- tracking of events.

A. Phantom Construction and Definition

Elements making up materials, utilized within the phantom geometry, would be defined by isotropic abundance. This provided the most accurate composition available and was obtained from an ICRU based program [8]; many of these compositions have been published elsewhere [13], [16]. The geometry was created utilizing right-angled parallelepiped (RPP) volumes depicting the spacecraft shield and layered homogeneous biologically important phantoms contained within the shield (Fig. 4). The spacecraft shield in this case would be represented by a 20 mm thick Al RPP volume that borders a 3000 mm air volume representing the astronaut's environment. Within this air volume a layered tissue equivalent (TE) phantom could be
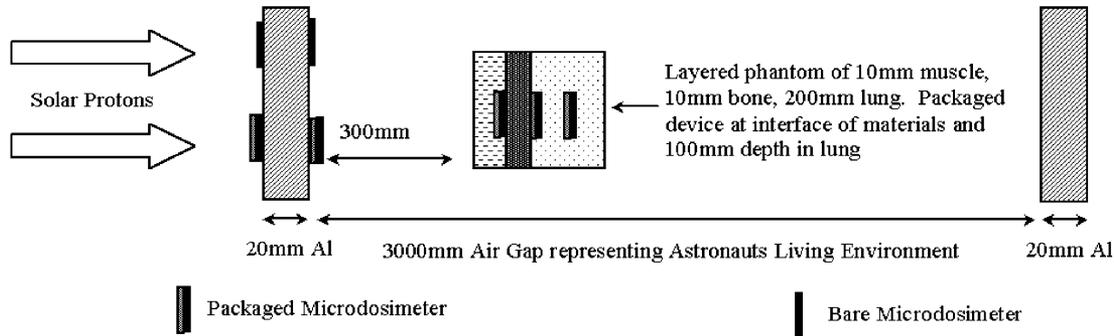
Fig. 4. Schematic representation of the simulated measurement positions of the SOI microdosimeter. It is important to note that for each simulation only one microdosimeter was present and as such separate simulations were conducted for each measurement position.

placed for microdosimetric studies of tissue interfaces when irradiated with solar protons.

The program was created such that five different RPP volumes of a given thickness could be created in front of the SOI microdosimeter, whilst an additional five volumes could follow the placement of the sensitive volume. This allowed the SOI microdosimeter to be placed at different positions within the phantom structure. It is important to note that for each simulation only one microdosimeter was present and as such separate simulations were conducted for each measurement position. The lateral dimensions of these phantoms were set arbitrarily to be twice those of the SOI microdosimeter, whilst the thickness of each volume is adjustable.

The silicon sensitive volume is modeled as a single RPP of dimensions $4800 \times 1600 \times 10 \ \mu m^3$ with charge collection efficiency of 0.8 as was derived in previous research [1]. The complicated device overlayer geometry is simplified to a 1 μm thickness SiO_2 layer. This device was then simulated as either a bare microdosimeter (i.e., without any further packaging) and as a packaged device. In the case of the packaged device further RPP volumes were added above the SiO_2 layer. These included a 300 μm air gap between SiO_2 layer and Perspex converter, along with a 3.5 mm Perspex converter and 0.4 mm thick aluminum shield.

B. Physics Processes and Incident Particles

The main component of any Monte Carlo program is the physics processes that are to be employed. In this case it was imperative that the process covered a number of different particles and energies. Low energy inelastic scattering, low energy ionization and multiple scattering models were employed for the transport of protons through the geometry of the simulation. The physics of secondary particles also needed to be considered and accounted for. In the case of alpha particles, deuterons, triton, and other generic charged ions produced as a result of inelastic proton interactions, the corresponding low energy inelastic scattering, low energy ionization and multiple scattering models would be utilized. The predominant particles generated within the simulation would be electrons resulting from proton ionization interactions. Electron processes supported included low energy ionization, low energy bremsstrahlung multiple scattering. In the event of photon generation, the physics processes included were low energy photoelectric effect, low energy Compton scattering, low energy Rayleigh scattering,

and low energy pair production. Neutron interactions were also accounted for using the appropriate models.

Incident protons whose energy would be dictated by a random sampling of the JPL solar proton spectra would be used as the incident particles in this simulation. An energy cut would be applied in order to allow for realistic simulation times. For simulations with the microdosimeter outside and immediately inside the spacecraft shield the entire JPL solar proton spectra would be sampled for incident particle energy. However, in the case of the microdosimeter being imbedded in the TE phantom only protons with energies exceeding 70 MeV would be considered, as those particles below such energies would not penetrate the 20 mm thick Al shield and contribute energy deposition events within the detector SV.

The position of the incident particles would randomly cover the entire cross sectional area of RPP volume representing the spacecraft shield with an initial direction perpendicular to this shield. A separate simulation of 10^6–10^8 (average 10^7) incident particles was carried out for each position of the SOI microdosimeter within the phantom structure.

C. Tracking of Events

In this simulation the array of silicon SVs of the SOI microdosimeter would be defined as the sensitive volume within the DetectorConstruction class of the program. All energy deposition events (whether from primary or secondary particles) within this volume would be tracked and the kinetic energy, charge and mass of the particle as well as the energy deposited within the SV were stored. Upon completion of the simulation within the RunAction class these events were then binned into a spectra of energy deposition events. A separate data analysis software program was then utilized to create the microdosimetry spectra from these results.

V. MICROSOMETRY SPRECTRA GENERATION

Energy depositions within the 10 μm SOI microdosimeter were scored generating an MCA spectra for conversion to a microdosimetry spectra according to the protocol outlined in ICRU report 36. A mean chord length of $\langle l \rangle = 19.05 \ \mu$m was used for these calculations. This value was based on a $30 \times 30 \times 10 \ \mu m^3$ volume and a tissue equivalent scaling factor of $\zeta = 0.6$
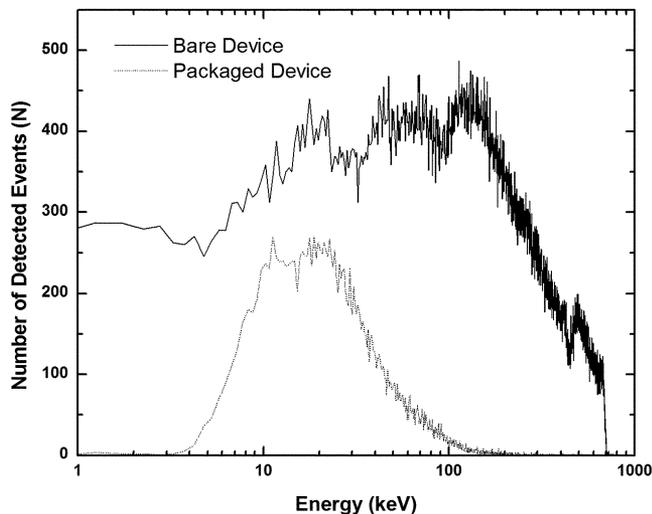
$$\langle l \rangle = \frac{4V}{S\zeta}$$

Fig. 5.   MCA spectra of the bare and packaged microdosimeters outside the spacecraft shield.

Fig. 6.   Microdosimetry spectra for both the packaged and bare microdosimeter outside and inside the shield.

where V is the volume, S is the total surface area, ζ is the equivalent scaling factor, $\langle l \rangle$ the mean chord length.

The spectra produced give the fraction of the total dose occurring from lineal energy events in the interval $y \rightarrow y + dy$.

VI. RESULTS AND DISCUSSION

The MCA spectra generated by the GEANT4 program in all cases was binned into 0.25 keV bins to provide accurate resolution for conversion to microdosimetric spectra. The simulations carried out with the microdosimeter both outside and just within the spacecraft shield registered interesting results.

It is clear from Fig. 5 that the small shielding present on the packaged device (i.e., 0.4 mm Al and 3.5 mm Perspex) is shielding the SV from most of the energy deposition events above 100 keV. The bare device however does not experience any shielding effect and as such the full spectra of protons (0.1–200 MeV) can deposit energy within the SV. There is also a significant reduction in the number of events experienced by the packaged device (approximately 15 times more events are detected by the bare device).

The bare device experiences energy deposition events of up to 700 keV. This corresponds to solar protons depositing their maximum energy within a 10 μm (thickness of the device) track within the SV [8] and is known as the proton edge. Events below 700 keV correspond to protons crossing or stopping within the SV and only depositing a fraction of the proton energy. It is important to note that some energy deposition events exceeding 700 keV were detected, however these were statistically very rare in this case (approximately 0.07% of energy deposition events exceeded 700 keV). Protons either obliquely striking the device, or experiencing scattering within the SV, increasing the mean chord length, cause the chord length to increase and hence result in an increase in the energy deposited within the SV.

In the case of these simulations all protons were normally incident upon the spacecraft shield, hence normally incident upon the SOI microdosimeter when mounted externally. As such no incident protons could strike the SV obliquely in the case of
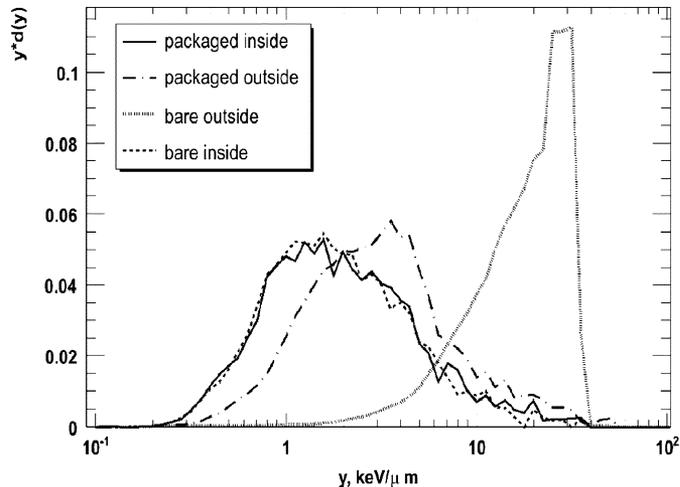
the bare microdosimeter (in the case of the packaged microdosimeter it is possible for the incident protons to be scattered by the device packaging). As such all events above 700 keV are attributed to internal scattering of protons causing $\langle l \rangle$ to be larger than 10 μm (thickness of the SV), hence allowing more than 700 keV to be deposited.

The MCA spectra generated by the GEANT4 simulations were converted to microdosimetry spectra in order to provide information on the quality of the radiation experienced by the device. Fig. 6 clearly demonstrates the effect of the higher energy depositions within the bare microdosimeter external to the spacecraft shield. This is a direct result of low energy solar protons depositing all or almost all their energy within the SV of the detector. This results in a very high dose weighted mean lineal energy of 21 keV/μm.

It is also important to note that in this case only 10^7 histories were simulated and this corresponds to a measurement of approximately 4.4 minutes (see Table I) in real time. Thus over a mission duration of 12 months or more, it is conceivable that external electronics exposed to these events would almost certainly undergo damage if not adequately shielded.

In contrast the packaged microdosimeter external to the spacecraft wall experiences a dose weighted mean lineal energy of 5.0 keV/μm. Whilst still relatively high, it clearly indicates the effectiveness of a small amount of shielding in reducing the damaging effect of solar protons. In this case the shielding present was 0.4 mm Al and 3.5 mm of Perspex and this was sufficient in removing the large portion of low energy protons, thus reducing the high lineal energy events that could conceivably damage or destroy the device.

Fig. 6 also clearly illustrates the effect of the spacecraft wall (20 mm Al) in filtering out the low energy proton incident on the spacecraft. Outside the spacecraft shield comparatively high dose weighted mean lineal energies of 21 and 5.0 keV/μm are experienced by the microdosimeter compared with 3.0 and 3.3 keV/μm inside the shield for the bare and packaged microdosimeters respectively. The comparatively low lineal energies of both the bare and packaged devices within the spacecraft shield indicate that the spacecraft shield of 20 mm

TABLE I
ACTUAL COLLECTION TIMES WITH RESPECT TO MISSION DURATION

	GEOMAGNITIC EFFECTS IGNORED	QUIET MAGNETOSHPERE GEOMAGNETIC EFFECTS CONSIDERED
TOTAL MISSION HISTORIES	1.20E+12	6.29E+10
NUMBER OF HISTORIES SIMULATED	1.00E+07	1.00E+07
FRACTION OF MISSION SIMULATED	8.36E-06	1.59E-04
COLLECTION TIME SECONDS	2.64E+02	5.02E+03
COLLECTION TIME MINUTES	4.39E+00	8.36E+01
COLLECTION TIME HOURS	7.32E-02	1.39E+00

Fig. 7. Microdosimetry spectra for the packaged microdosimeter within the three layers of the TE phantom.

Al is suitable for not only removing a large portion of low energy protons, but do so without producing a large amount of high LET secondary particles that could be damaging to not only electronics but also the astronauts within the capsule.

These results do however highlight an important fact concerning operational deployment of the SOI microdosimeter for radiation protection purposes in space. In operational deployment SOI microdosimeters will need different packaging for different purposes. In this study it is clear that in order to detect low energy protons (such as solar protons) the packaging of the device should be minimal to be able to accurately measure the solar proton environment outside the spacecraft (as was seen in the case of the bare microdosimeter in this study). However, the radiation spectra of space is not only represented by solar protons. In the case of deep space travel GCR consisting of neutrons will be experienced. As such a monitoring device such as the SOI microdosimeter will need a converter in order to be able to detect such particles. As such it is recommendable that a number of SOI devices both outside and inside the spacecraft shield be present with different packaging configurations to allow for the accurate measurement of the range of particles present in space.

Another point of discussion is the cross sectional area of the SOI microdosimeter and if it is sufficient to obtain a statistically acceptable result in an acceptable timeframe to be a monitor for astronaut safety (i.e., detect adverse radiation conditions in time for the personnel to move into a shelter radiation shelter on the spacecraft). In this case the average number of histories simulated was 10^7, which corresponded to a measurement of 4.4 minutes when disregarding geomagnetic effects and a measurement time of 1.4 hours when we consider geomagnetic effects within a quiet magnetosphere. The cross sectional area of the device (i.e., $4800 \times 1600 \ \mu m^2$) is sufficient in obtaining real time radiation protection as one could expect a 4-minute window before the device would register abnormal radiation readings allowing the personnel to take the appropriate steps.

It is also conceivable that such a device can be used for long-term monitoring of personnel deployed on missions by conversion of the microdosimetric spectra to TE microdosimetric spectra. Such a conversion would be achieved by applying a conversion factor of 0.62. The ability of the device to get statistically significant results in hours (i.e., 1.4 hours in a quiet magnetosphere within the spacecraft wall) will make it applicable to short missions as well as longer missions where the
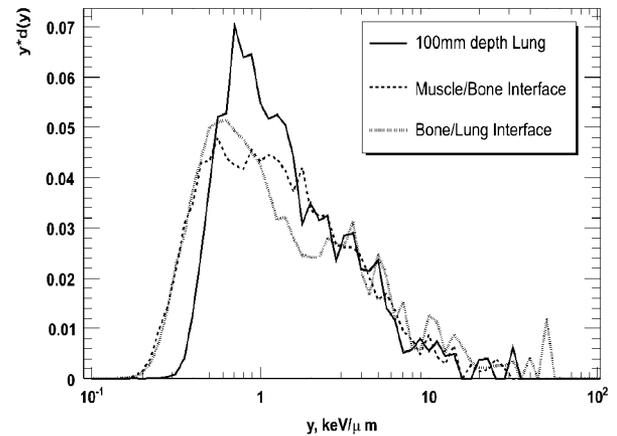
spacecraft will encounter higher levels of radiation and GCR in addition to solar protons.

Fig. 7 gives the change in microdosimetric spectra within the different layers of a TE phantom constructed to represent the chest wall of an astronaut. Such events are a result of higher energy protons traversing the Al shielding of the spacecraft and being detected by the SOI microdosimeter imbedded at the muscle/bone and bone/lung interfaces and at 100 mm depth within the lung phantom.

The dose weighted mean lineal energies in the case of muscle/bone and bone/lung interfaces are 2.3 and 3.2 keV/μm respectively. This illustrates the increased biological effectiveness of the radiation with depth in the phantom, and the higher probability for inelastic reaction especially for bone. The higher lineal energies experienced after a hard boundary such as bone are a direct result of due to higher LET protons and inelastic products produced within the bone and could result in increased tissue damage immediately after such a boundary. These higher instances of cellular damage could have a knock-on effect, resulting in higher instances of cancer in the tissue located at such a boundary.

The spectrum obtained for the microdosimeter situated in the lung phantom shows a further shift in the peak position to higher lineal energies, reflecting the further decrease in protons energy with depth. The contribution of proton events to the total dose is higher than for the previous two microdosimeter positions and this may be attributed to the decreased probability of inelastic interactions in the lower density lung medium. The dose weighted mean lineal energy at this position is 2.5 keV/μm. The radiobiological effect of the proton radiation thus varies in different tissue substances, which is observable through changes in dose weighted mean lineal energy.

VII. CONCLUSION

This GEANT4 simulation study simulated the response of the SOI microdosimeter that has been produced by Fujitsu and developed at the Centre for Medical Radiation Physics, University of Wollongong. The device was irradiated by a spectra of solar protons that was sourced from the SPENVIS [8] website using the JPL model to a 95% confidence level for the international

space station. The SOI microdosimeter was simulated in both is bare and packaged state external and directly inside the space-craft shield (represented by 20 mm Al) and also within a layered TE phantom.

In viewing the MCA spectra obtained from the bare micro-dosimeter outside the spacecraft shield the microdosimetric edge corresponding to maximum proton energy being deposited within the 10 μm thickness of the microdosimeter (i.e., approximately 700 keV). Events below 700 keV correspond to protons crossing or stopping within the SV and only depositing a fraction of the proton energy.

It was clear from the simulations of the bare and packaged microdosimeters inside and outside the spacecraft wall that the spacecraft wall removed a large degree of solar protons without generating a large amount off secondaries. Outside the space-craft shield comparatively high dose weighted mean lineal energies of 21 and 5.0 keV/μm are experienced by the micro-dosimeter compared with 3.0 and 3.3 keV/μm inside the shield for the bare and packaged microdosimeters respectively. Such high lineal energies outside the shielding are a direct result of the low energy protons depositing all their energy within the SV. Differences in results especially outside the spacecraft between the packaged and bare device can be attributed to the filtering of low energy protons by the device packaging.

The results obtained from these simulations represented a time period of approximately 4.4 minutes, hence demonstrating the adequacy of the SOI microdosimeter in providing online warning system for astronauts to adverse radiation conditions. The microdosimeter could also be used for long-term monitoring of personnel deployed on missions by conversion of the microdosimetric spectra to TE microdosimetric spectra. The ability of the device to get statistically significant results in hours (i.e., 1.4 hours in a quiet magnetosphere within the spacecraft wall) will make it applicable to short missions as well as longer missions where the spacecraft will encounter higher levels of radiation and GCR in addition to solar protons. For such missions different packaging structures would be utilized to enable the sampling of different particles.

By simulating the microdosimetric spectra within the different layers of a TE phantom constructed to represent the chest wall of an astronaut it was possible to demonstrate the change in microdosimetric spectra within different material. At hard boundaries such as immediately after a bony landmark it is conceivable that the higher dose weighted mean lineal energy will result in a higher degree of cell damage and thus a higher probability of cancer formation within soft tissues immediately following such a structure.

VIII. FURTHER WORK

With the SOI microdosimeter set to be deployed as silicon microdosimetric sensors on the MidSTAR-I spacecraft experimental results will able to be obtained on the microdosimetric spectra of an orbiting satellite. These will be further compared to simulation results of the radiation field for the given orbit parameters. Such work will further profess the applicability of the SOI microdosimeter as a monitoring system for astronauts and the electrical equipment located within the spacecraft.

Simulation studies using GEANT4 of the RBE of field in each organ based on derived microdosimetric spectra and $Q(y)$ factor will also be completed. These will be compared with the fluence-based method for cancer induction. Such work will provide an assessment of both methods for space applications.

REFERENCES

[1] P. D. Bradley, A. B. Rosenfeld, and M. Zaider, "Solid state microdosimetry (Invited Paper)," *Nucl. Instrum. Methods Phys. Res. B* , vol. 184, pp. 135–157, 2001.

[2] J. F. Dicello, H. I. Amols, M. Zaider, and G. Tripard, "A comparison of microdosimetric measurements with spherical proportional counters and solid-state detectors," *Radiat. Res.*, vol. 82, pp. 441–453, 1980.

[3] T. Ersmark *et al.*, "Status of the DESIRE project: Geant4 physics validation studies and first results from Columbus/ISS radiation simulations," *IEEE Trans. Nucl. Sci.*, vol. 51, no. 4, pp. 1378–1384, Aug. 2004.

[4] S. Agostinelli and Geant4 Collaboration, "GEANT4: A simulation toolkit," *Nucl. Instrum. Methods Phys. Res. A*, vol. 506, pp. 250–303, 2003.

[5] "Microdosimetry," Int. Commission on Radiation Units and Measurements, Bethesda, MD, Dec. 1983. ICRU Rep. 36.

[6] F. Lei *et al.*, "MULASSIS: A Geant4-based multilayered shielding simulation tool," *IEEE Trans. Nucl. Sci.*, vol. 49, no. 6, pp. 2788–2793, Dec. 2002.

[7] P. J. McNulty, D. R. Roth, W. J. Beauvois, W. G. Abdel-Kader, and E. G. Stassinopoulos, "Microdosimetry in space using microelectronic circuits," in *Proc. NATO-ASI on Biological Effects and Physics of Solar and Galactic Cosmic Radiation*, Armacaco de Pera, Portugal, 1991.

[8] National Institute of Standards and Technology (NIST) PSTAR database program [Online]. Available: http://physics.nist.gov/cgi-bin/Star/compos.pl?ap

[9] V. L. Pisacane, J. F. Ziegler, A. B. Rosenfeld, M. Zaider, M. E. Nelson, and J. F. Dicello, "MIDN: A spacecraft microdosimetry mission," *Rad. Prot. Dosim.*, to be published.

[10] J. Robertson, J. Eaddy, J. Archambeau, G. Coutrakon, D. Miller, M. Moyers, J. Siebers, J. Slater, and J. Dicello, "Relative biological effectiveness and microdosimetry of a mixed energy field of protons up to 200 MeV," *Adv. Space Res.*, vol. 14, no. 10, pp. 217–275, 1994.

[11] A. B. Rosenfeld, G. I. Kaplan, M. G. Carolan, B. J. Allen, R. Maughan, M. Yudelev, C. Kota, and J. Coderre, "Simultaneous macro-micro dosimetry with MOSFETs," *IEEE Trans. Nucl. Sci.*, vol. 43, no. 6, pp. 2693–2700, 1996.

[12] A. B. Rosenfeld, P. D. Bradley, I. Cornelius, M. Zaider, R. Maughan, J. Flanz, J. Yanch, T. Kobayashi, and B. J. Allen, "Microdosimetry in hadron therapy," *Rad. Prot. Dosim.*, vol. 101, no. N1/4, pp. 431–434, 2002.

[13] A. B. Rosenfeld, A. J. Wroe, I. M. Cornelius, M. Reinhard, and D. Alexiev, "Analysis of inelastic interactions for therapeutic proton beams using Monte Carlo simulation," *IEEE Trans. Nucl. Sci.*, vol. 51, no. 6, pp. 3019–3025, 2004.

[14] J. A. Simpson, "Introduction to the galactic cosmic radiation," in *Composition and Origin of Cosmic Rays*, M. M. Shapiro, Ed. Dordrecht, The Netherlands: Reidel Publishing, 1983.

[15] SPENVIS website [Online]. Available: http://www.spenvis.oma.be/spenvis/

[16] A. J. Wroe, I. M. Cornelius, and A. B. Rosenfeld, "The role of nonelastic reactions in absorbed dose distributions from therapeutic proton beams in different medium," *Med. Phys.*, vol. 32, no. 1, pp. 37–41, 2005.